



CHORUS

This is the accepted manuscript made available via CHORUS. The article has been published as:

Quantum algorithm for obtaining the energy spectrum of a physical system

Hefeng Wang, S. Ashhab, and Franco Nori

Phys. Rev. A **85**, 062304 — Published 5 June 2012

DOI: [10.1103/PhysRevA.85.062304](https://doi.org/10.1103/PhysRevA.85.062304)

Quantum algorithm for obtaining the energy spectrum of a physical system

Hefeng Wang^{1,2,3}, S. Ashhab^{2,3}, and Franco Nori^{2,3}

¹*Department of Applied Physics, Xi'an Jiaotong University, Xi'an 710049, China*

²*Advanced Science Institute, RIKEN, Wako-shi, Saitama 351-0198, Japan*

³*Department of Physics, The University of Michigan, Ann Arbor, Michigan 48109-1040, USA*

We present a polynomial-time quantum algorithm for obtaining the energy spectrum of a physical system, i.e. the differences between the eigenvalues of the system's Hamiltonian, provided that the spectrum of interest contains at most a polynomially increasing number of energy levels. A probe qubit is coupled to a quantum register that represents the system of interest such that the probe exhibits a dynamical response only when it is resonant with a transition in the system. By varying the probe's frequency and the system-probe coupling operator, any desired part of the energy spectrum can be obtained. The algorithm can also be used to deterministically prepare any energy eigenstate. As an example, we have simulated running the algorithm and obtained the energy spectrum of the water molecule.

PACS numbers: 03.67.Ac, 03.67.Lx

I. INTRODUCTION

Obtaining the energy spectrum of a physical system is an important task in a variety of fields. In general, one has to solve the Schrödinger equation of the system, which is a difficult task on a classical computer for large systems, because the dimension of the Hilbert space of the system increases exponentially with the size of the system, which is commonly defined as the number of particles in the system. Thus, the complexity of simulating the quantum system grows exponentially. On a quantum computer, however, the number of qubits required to simulate the system increases linearly with the size of the system. As a result, Solving the Schrödinger equation of the system is more efficient on a quantum computer than on a classical computer [1–5].

The standard quantum algorithm for obtaining the eigenvalues and eigenvectors of the Hamiltonian of a quantum system is the phase estimation algorithm (PEA) [6–13]. In the PEA, one prepares an initial guess state, and the algorithm randomly “selects” one of the energy eigenstates in the guess state and produces its energy as the output of the algorithm. It is worth mentioning here that the probability of selecting a given energy eigenstate is equal to the square of its overlap with the guess state. In reality, one is usually most interested in the energy differences between energy levels, instead of the absolute energy of a given energy level. In this paper, we present a quantum algorithm that solves this problem: obtaining the energy differences between energy levels of a quantum system described by a given Hamiltonian. The algorithm can also be used to prepare any energy eigenstate of the system.

Our algorithm is motivated by the following observation in simulating the dynamics of an open quantum system [14–16]: For an open system interacting with many environment modes, the mode that resonates with a certain transition in the spectrum of the open system contributes the most to the decay dynamics associated with that transition. This property suggests a method to locate the transition frequencies separating the different energy levels of a physical system.

The basic idea of the algorithm is as follows: we couple the quantum system to a probe qubit with a certain frequency, set the probe qubit in one of its energy eigenstates (say the excited state), evolve the whole system for some time, then perform a measurement on the probe qubit. When the frequency of the probe qubit matches the transition frequency between two energy levels of the quantum system, one observes a peak in the decay rate of the probe qubit. Therefore by varying the frequency of the probe qubit, we can locate the transition frequencies of the quantum system. We can also set the probe qubit to be in its ground state and measure its excitation dynamics. The difference is that in the former case we obtain the absorption spectroscopy of the system while in the latter case we obtain the emission spectroscopy.

This algorithm has the following advantages: (i) There are several adjustable elements (initial state of the system, interaction operator, evolution time and system-probe coupling strength) that can be varied in order to improve the efficiency of the algorithm. (ii) The coupling of the system to the probe qubit can simulate a realistic interaction, and therefore the algorithm can naturally identify transitions that would occur in a realistic setting. (iii) Because of the freedom associated with choosing the coupling operator, the algorithm gives as an additional piece of output the transition matrix elements for any desired operator. (iv) Because the algorithm involves transitions between different energy eigenstates, preparing the system in a good approximation to any particular energy eigenstate is less crucial than in the phase estimation algorithm.

The structure of this work is as follows: In Sec. II, we present an algorithm for simulating the dynamics of an open

quantum system. In Sec. III, we estimate the resource requirements for the algorithm. In Sec. IV, we discuss the efficiency, the accuracy and the resource requirement of the algorithm, and compare our algorithm with the PEA. We close with a conclusion section.

II. THE ALGORITHM

First, we make an initial guess about the range of the energy differences between the energy levels of the system, $[\omega_{\min}, \omega_{\max}]$. We discretize this frequency range into j intervals, where each interval has a width of $\Delta\omega = (\omega_{\max} - \omega_{\min})/j$, and the center frequencies are given by $\omega_k = \omega_{\min} + (k + 1/2)\Delta\omega, k = 0 \dots, j - 1$. We now let a probe qubit couple to the quantum system, and we design the Hamiltonian of the whole system to be of the form

$$H = H_S + \frac{1}{2}\omega\sigma_z + cA \otimes \sigma_x, \quad (1)$$

where the first term is the Hamiltonian of the system, the second term is the Hamiltonian of the probe qubit, and the third term describes the interaction between the system and the probe qubit. Here, ω is the frequency of the probe qubit (we have set $\hbar = 1$), and c is the coupling strength between the probe qubit and the system, while σ_x and σ_z are Pauli matrices. The operator A acts in the state space of the system and plays the role of an excitation operator that transfers the initial state of the quantum system to another state. The frequency ω is taken from the frequency set ω_k . For a frequency ω_k of the probe qubit, we let the whole system evolve with the Hamiltonian shown in Eq. (1) for a time τ . This evolution is implemented using the procedure of quantum simulation based on the Trotter-Suzuki formula [17]. After that, we read out the state of the probe qubit. We repeat the whole procedure many times in order to obtain the decay probability. Then we change the probe frequency and repeat this procedure until we cover all the frequencies in the range $[\omega_{\min}, \omega_{\max}]$.

Setting the probe qubit in its excited (ground) state, when the frequency of the probe qubit matches the transition frequency between two energy levels of the quantum system, the probe qubit has the fastest decay (excitation). For example, in the case where the initial state of the probe qubit is the excited state, the final state of the probe qubit is:

$$\rho_p(\tau) = \text{Tr}_S[U(\tau) (|\psi_s\rangle\langle\psi_s| \otimes |1\rangle\langle 1|) U^\dagger(\tau)], \quad (2)$$

where $\text{Tr}_S[\dots]$ means tracing out the system degrees of freedom. The unitary evolution operator $U(\tau) = \exp(-iH\tau)$, H is given in Eq. (1), $|\psi_s\rangle$ is the initial state of the system, and $|1\rangle$ represents the excited state of the probe qubit, while $|0\rangle$ represents the ground state of the probe qubit. The quantity of interest to us now is the decay probability of the probe qubit $P_{\text{decay}} = \langle 0|\rho_p(\tau)|0\rangle$. By plotting P_{decay} as a function of the probe-qubit frequency, we can obtain the absorption spectrum of the system. If there are no degeneracies in the transition frequencies, at most one transition (denoted by $i \rightarrow j$) in the system will contribute to the decay dynamics of the probe qubit (taking into consideration the possibility of degenerate transitions makes the derivations longer but does not affect our main results). In this case, we obtain the result

$$P_{\text{decay}} = \sin^2\left(\frac{\Omega_{ij}\tau}{2}\right) \frac{Q_{ij}^2}{Q_{ij}^2 + (E_j - E_i - \omega_k)^2} |\langle\varphi_i|\psi_s\rangle|^2, \quad (3)$$

where $Q_{ij} = 2c|\langle\varphi_j|A|\varphi_i\rangle|$, and $\Omega_{ij} = \sqrt{Q_{ij}^2 + (E_j - E_i - \omega_k)^2}$. $|\varphi_i\rangle$ is the i -th energy eigenstate of the system and E_i is the corresponding eigenenergy. Eq. (3) describes Rabi-oscillation dynamics, where the system and probe exchange an excitation. The second factor on the right-hand side is the maximum oscillation probability, and it depends on the relation between the matrix element for a given transition and the system-probe detuning for that transition. The third factor is the overlap between the initial state of the system and a given energy eigenstate.

In general, the interaction between the probe qubit and the quantum system should be weak such that the widths of the peaks are small and one obtains accurate results. The evolution time τ should ideally be large ($c\tau \sim 1$), such that the change of the system is clear and the peaks in the spectroscopy have high resolution.

The procedure of the algorithm is as follows: (i) prepare a quantum register R_S , which encodes the state of the system, in state $|\psi_s\rangle$, and the probe qubit in state $|1\rangle$; (ii) implement the unitary operator $U(\tau) = \exp(-iH\tau)$ where H is given in Eq. (1); (iii) read out the state of the probe qubit; (iv) perform steps (i) – (iii) many times in order to obtain good statistics and calculate the decay probability; (v) repeat steps (i) – (iv) for different frequencies of the probe qubit. From the above procedure, one obtains the absorption spectroscopy of the system. One can also set the probe qubit in its ground state $|0\rangle$, and perform the above steps in order to obtain the emission spectroscopy. The quantum circuit for steps (i) – (iii) is shown in Fig. 1.

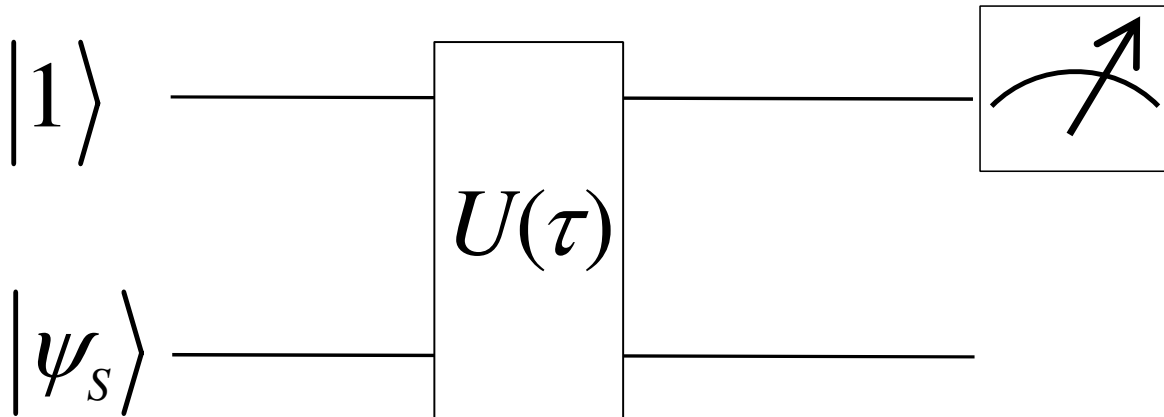


FIG. 1: Quantum circuit for obtaining the energy spectrum of a physical system. The first input register represents a probe qubit, and the second input register represents the system whose spectrum we are trying to obtain.

III. EXAMPLE: OBTAINING THE ENERGY SPECTRUM OF THE WATER MOLECULE

In the following, we present an example that demonstrates how the algorithm would perform in obtaining the energy spectrum of the water molecule.

To apply the quantum algorithm presented above, first we have to map the state space of the water molecule to the state space of the qubits. Using the mapping technique introduced in Ref. [9], considering the C_{2V} and 1A_1 symmetries known from quantum chemistry of the water molecule, we can minimize the number of qubits needed to represent the water molecule on a quantum register. Note that the symmetries can be used with the PEA in order to optimize the algorithm in the same way that we have used them in the water-molecule example. These symmetries would not lead to an exponential speedup in either algorithm. In other words, knowing the symmetries is not crucial for running the algorithm and for having a polynomial scaling of resources. The Hamiltonian for water molecule is given in Ref. [18] and shown below. The Hartree-Fock wave function for the ground state of the water molecule is $(1a_1)^2(2a_1)^2(1b_2)^2(3a_1)^2(1b_1)^2$. Using the STO-3G basis set [18] and freezing the first two a_1 orbitals, we construct a model space with 1A_1 symmetry that includes the $3a_1, 4a_1, 1b_1$ and $1b_2$ orbitals and we consider only single and double excitations to the external space for performing the multi-reference-configuration interaction (MRCI) calculation. The MRCI space is composed of 18 configuration state functions. Therefore at least 5 qubits are required to represent the state of the water molecule in this calculation.

In order to optimize the implementation of the algorithm, it is useful to have a priori knowledge of the molecular states and their symmetries. This can be done using quantum-chemistry algorithms on a classical computer.

The Hamiltonian of the water molecule in the form of second quantization is

$$H = \sum_{p,q} \langle p | T + V_N | q \rangle a_p^\dagger a_q - \frac{1}{2} \sum_{p,q,r,s} \langle p | \langle q | V_e | r \rangle | s \rangle a_p^\dagger a_q^\dagger a_r a_s, \quad (4)$$

where $|p\rangle$ is the one-particle state, a_p^\dagger is its fermionic creation operator, and T , V_N , and V_e are the one-particle kinetic operator, nuclear attraction operator and the two-particle electron repulsion operator, respectively.

For the initial state, we prepare the system register in the simple state $|00010\rangle$, which is close to the true ground state. Then we implement the unitary operation $U = \exp(-iH\tau)$. For the interaction operator A , we set

$$A = (A_1 + A_2 + A_3 + A_4 + A_5)/\sqrt{5}, \quad (5)$$

where $A_1 = I \otimes I \otimes I \otimes I \otimes \sigma_x$, $A_2 = I \otimes I \otimes I \otimes \sigma_x \otimes I$, $A_3 = I \otimes I \otimes \sigma_x \otimes I \otimes I$, $A_4 = I \otimes \sigma_x \otimes I \otimes I \otimes I$, $A_5 = \sigma_x \otimes I \otimes I \otimes I \otimes I$. We set the coupling strength $c = 0.005$ and the evolution time $\tau = 500$ (here we measure energies in units of Hartree and time in units of Hartree $^{-1}$). We vary the frequency of the probe qubit in the range $\omega \in [0.4, 2.0]$, which is divided into 200 intervals, and run the circuit shown in Fig. 1. We obtain the spectrum shown in Fig. 2 for the transition frequencies between the ground state and several excited states. From the figure we can see

that the spectroscopy obtained using our algorithm is in very good agreement with the known transition frequency spectrum (in red) of the water molecule.

The coupling strength c and the evolution time τ can be adjusted to improve the resolution of the peaks and the accuracy of the results. In order to demonstrate this point, we now set $c = 0.001$ and $\tau = 2500$. We focus on the second and the third peaks as shown in the inset of Fig. 2. We can see that the widths of the peaks are reduced and the resolution of the peaks is now higher. We also observe a small peak at the frequency of the transition between the second and the eighth energy levels.

From Fig. 2, we can see that some transitions between the ground state and the excited states are barely visible. Their decay probabilities can be improved by constructing a different operator A . The choice for the operator A in Eq.(5) includes single-qubit operators with all the qubits represented. With this choice most of the desired resonance peaks are observed in the simulation. However, as can be seen in Fig.2, some peaks are very low. We use two-qubit operators in Eq. (6) in order to look for any such ‘‘missing’’ peaks. In fact, we have tried a few different choices, and we only show the one that resulted in all the peaks being visible. In principle, even if no single operator (as happened in our example) produces all the resonance peaks, one can still construct the spectrum by putting together the information obtained from the different choices for A . We define the operators $A_6 = I \otimes I \otimes I \otimes \sigma_x \otimes \sigma_x$ and $A_7 = I \otimes I \otimes \sigma_x \otimes \sigma_x \otimes I$, set the interaction operator

$$A = (A_1 + A_2 + A_3 + A_6 + A_7)/\sqrt{5}, \quad (6)$$

and run the algorithm. The results are shown in Fig. 3. We can see that now all the expected peaks are clearly visible.

In our algorithm, we can transfer the initial state of the system to another state through the interaction operator A . Therefore the initial state of the system is not of crucial importance to the success of the algorithm. Here we give an example that demonstrates how the PEA can fail when the initial state is not a good approximation of the desired state, but where our algorithm still succeeds.

In the PEA, the success probability of the algorithm depends on the overlap of the initial guess state with the exact eigenstate of the system. In the previous example, if the initial state of the water molecule is prepared in state $|11111\rangle$, the overlap of this state with any of the 18 eigenstates of the water molecule is *zero*. Therefore the PEA will *fail* in such a case. Our algorithm, however, still works.

We set the operator A to be

$$A = \frac{1}{3} \sum_{i=1}^9 B_i, \quad (7)$$

where $B_1 = \sigma_x \otimes \sigma_x \otimes \sigma_x \otimes \sigma_x \otimes I$, $B_2 = \sigma_x \otimes \sigma_x \otimes \sigma_x \otimes I \otimes \sigma_x$, $B_3 = \sigma_x \otimes \sigma_x \otimes I \otimes \sigma_x \otimes \sigma_x$, $B_4 = \sigma_x \otimes I \otimes \sigma_x \otimes \sigma_x \otimes \sigma_x$, $B_5 = \sigma_x \otimes \sigma_x \otimes \sigma_x \otimes I \otimes I$, $B_6 = \sigma_x \otimes I \otimes I \otimes \sigma_x \otimes \sigma_x$, $B_7 = \sigma_x \otimes I \otimes \sigma_x \otimes I \otimes I$, $B_8 = \sigma_x \otimes I \otimes I \otimes I \otimes \sigma_x$, $B_9 = \sigma_x \otimes \sigma_x \otimes \sigma_x \otimes \sigma_x \otimes \sigma_x$. And using the state $|11111\rangle$ as the initial state of the system. We set the coupling coefficient $c = 0.002$, and the evolution time $\tau = 800$, and run the algorithm. The results are shown in Fig. 4. From this figure we can see that the algorithm still has a high success probability in obtaining the energy spectrum of the water molecule.

IV. DISCUSSION

In the following, we discuss the factors that affect the efficiency, the accuracy and the resource requirements of the algorithm, and we compare our algorithm with the phase estimation algorithm.

The efficiency of the algorithm is most naturally defined through the number of times that the circuit in Fig. 1 must be run in order to identify the peaks in the spectrum. This number is proportional to the number of frequency points that need to be used and the number of times that the circuit needs to be run for a single frequency. Most physical systems have typical energy scales that are linear in the system size (for the total energy), while some unusual systems exhibit a polynomial dependence with relatively small exponents. The energy scale for the low-energy spectrum might be even smaller than that scale. The number of frequency points that need to be used in the algorithm, which is proportional to the frequency range, therefore scales polynomially with the system size. The number of times that the circuit needs to be run for a single frequency must be at least proportional to $1/P_{\text{decay}}$ in order to observe a peak. It should also be mentioned here that each single run of the algorithm is essentially a quantum simulation of the dynamics, which scales polynomially with the size of the system [19].

We note here that, for large systems, there is an exponentially large number of energy eigenstates, and determining the entire spectrum of a large system exhibits exponential complexity. However, one is usually not interested in all of

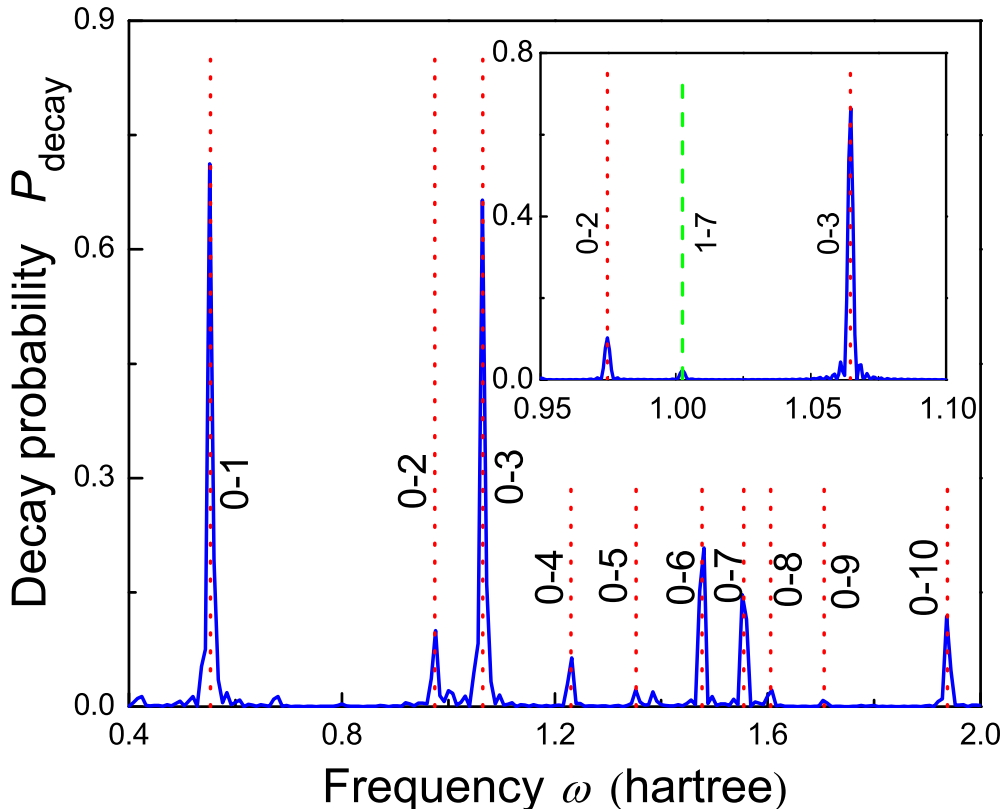


FIG. 2: (Color online) Transition frequency spectrum between the ground state, $|\varphi_0\rangle$, and the first ten excited states ($|\varphi_i\rangle, i = 1, 2, \dots, 10$) of the water molecule. The blue solid curve represents the decay probability of the probe qubit at different frequencies with the coupling coefficient in Eq. (1) $c = 0.005$ and the evolution time $\tau = 500$, and the operator A as shown in Eq. (3). The red dotted vertical lines represent the known transition frequencies between the ground state and the first ten excited states of the water molecule. In the inset, the second and the third transition frequencies shown in blue were obtained using $c = 10^{-3}$ and $\tau = 2500$. The green vertical dashed line represents the known transition frequency (1-7) between the first and the seventh excited states.

the energy eigenstates, but rather a very small fraction of them, that is, polynomially number of energy eigenstates. The energy eigenstates of interest could for example be the low-lying energy levels or the energy levels that are connected with the ground state by strong electric-dipole transitions. Once the criterion for the “energy levels of interest” is specified, and their number is small (or at least not exponentially large), the complexity of the algorithm does not grow exponentially with the size of the system any more. The part of the spectrum of interest will appear naturally in our algorithm, because the system will undergo transitions that mimic those of the simulated system.

Since the heights of the peaks depend on the product $\Omega_{ij}\tau$, we assume as a “worst-case scenario” that $Q_{ij}\tau \ll 1$ and find that the decay probability in Eq. (3) at the center of a given peak (i.e. at $\omega_k = E_j - E_i$) can be approximated as

$$P_{\text{decay}} \approx c^2 \tau^2 |\langle \varphi_j | A | \varphi_i \rangle|^2 |\langle \varphi_i | \psi_s \rangle|^2. \quad (8)$$

From the above equation, we can see that the decay probability, and therefore the efficiency of the algorithm, depends on the coupling strength, the evolution time, the interaction operator and the initial state of the system. Note that we can also use a number of qubits in parallel as probe qubits in order to improve the efficiency of the algorithm. We now address the roles of the different factors appearing in Eq. (6).

The parameters c and τ define the accuracy of the algorithm. The accuracy is given by the width of the peaks, and this width is given by $\max [c \langle \varphi_j | A | \varphi_i \rangle, 1/\tau]$ [15]. To obtain accurate results, we need to set c to be small so that we have weak system-probe coupling and the evolution time τ is set to be large such that the change of the system

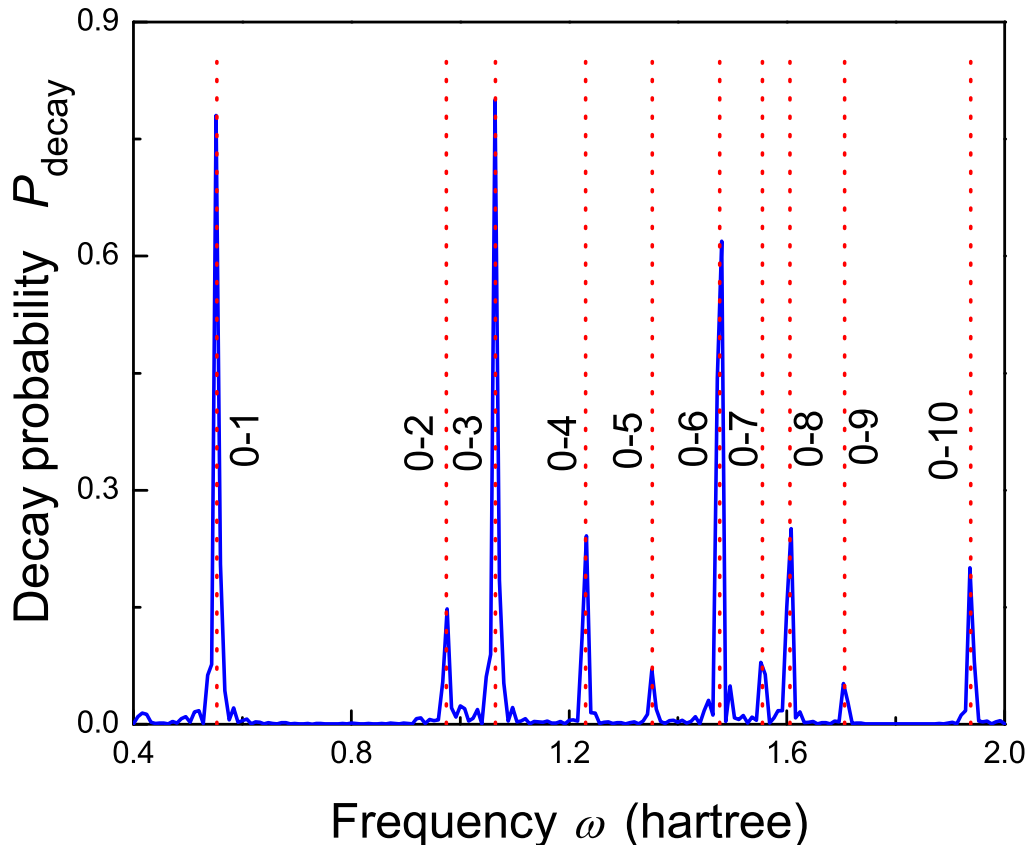


FIG. 3: (Color online) Same as in Fig. 2, except the operator A is set as shown in Eq. (4).

remains observable. Note that the accuracy is set by the experimenter, independently of the size of the system. It is also worth noting here that the size of the frequency intervals $\Delta\omega$ is set by the choice of c and τ : $\Delta\omega$ should be smaller than the width of the peaks in order to avoid missing some of the peaks, but there is no point in reducing $\Delta\omega$ far beyond this point.

Since P_{decay} depends on $\langle\varphi_j|A|\varphi_i\rangle$, the algorithm can also be used to obtain the matrix element $\langle\varphi_j|A|\varphi_i\rangle$ for any operator A and any two energy eigenstates, provided that this matrix element is not exponentially small. For this purpose, it would be ideal to set the initial state to one of the states $|\varphi_i\rangle$, which can be achieved as will be explained shortly. One can then use the height of the peak to obtain $\langle\varphi_j|A|\varphi_i\rangle$. In this context it is also worth noting that since the height of the peak depends on $\langle\varphi_j|A|\varphi_i\rangle$, certain transitions might not result in any peaks if the relevant matrix element vanishes. By designing A to be a physically-relevant operator, e.g. the operator that describes the coupling of a molecule to an electric field, one can identify transitions that would occur under electromagnetic irradiation of a molecule. Needless to say, A is not restricted to be a naturally occurring operator.

The last factor in Eq. (6) is the overlap between the initial state and any given energy eigenstate (which serves as the initial state in a given transition). In principle, preparing an initial state that has a large overlap with any given energy eigenstate can be a difficult task, possibly involving exponential scaling in the size of the system. However, a crucial point here is that once we observe a transition at the end of given run of the algorithm, we know that the final state of the system is the final energy eigenstate of the relevant transition. We can now use this state as the new initial state and rerun the algorithm. If the new initial state is different from a state that we wish to examine, we can convert the state of the system into the desired state by adding or subtracting from the system the required energy difference, which we would know at least approximately. Even if the two states in question were macroscopically different, it should be possible to go from one of them to the other via an at-most polynomially large number of transitions each of which involves single- or few-body operators. In many cases of practical interest, a relatively small number of transitions are needed to connect the energy levels of interest, e.g. the low-lying energy eigenstates.

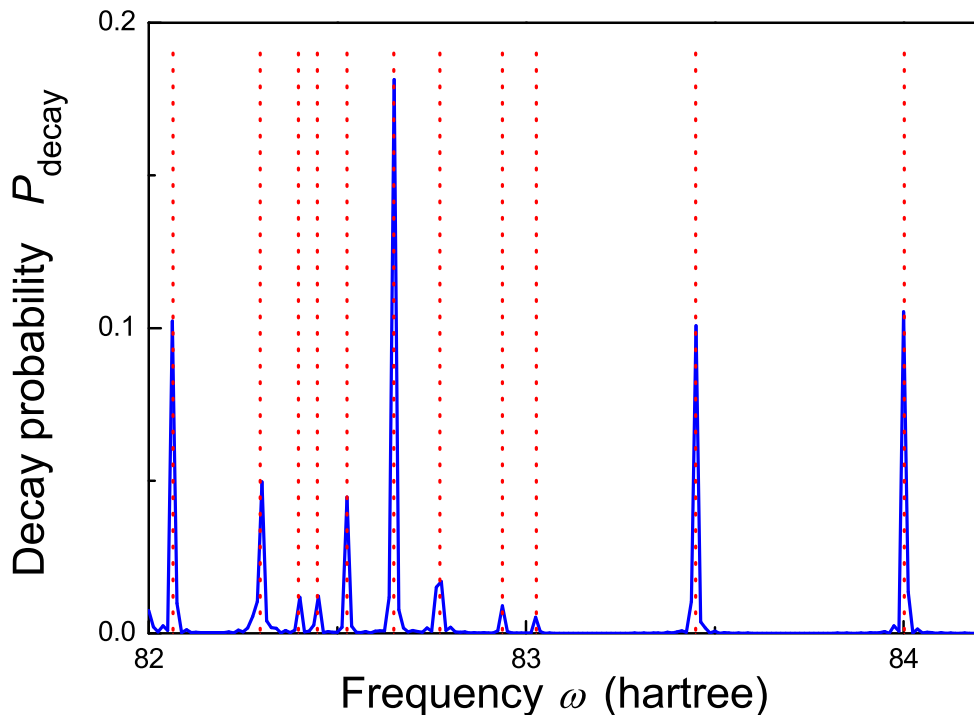


FIG. 4: (Color online) Transition frequency spectrum between the first 11 eigenstates of the water molecule and the state $|11111\rangle$. The blue solid curve represents the decay of the probe qubit at different frequencies with the coupling coefficient shown in Eq. (1) $c = 0.002$ and the evolution time $\tau = 800$ and operator A as shown in Eq. (5), in simulating the algorithm, and the red dotted vertical line represents the known eigenenergies of the first 11 eigenstates of the water molecule.

We note here that, since our algorithm relies on changes in the energy to keep track of the state of the system, one cannot tell whether a given energy level is degenerate or not, and in the case of degeneracy one cannot tell which final state is obtained upon detecting the relevant transition. If one wishes to check for degeneracies, one could add a few small perturbations to the Hamiltonian of the system, and for most physical systems these perturbations will lift the degeneracies in the spectrum.

Finally, we compare our algorithm with the PEA. In the PEA, one prepares an initial state that ideally has a large overlap with the desired energy eigenstate, and the algorithm produces the energy of that state. In cases where the desired energy eigenstate has a complicated form or whose form is unknown, it can become impossible to prepare a guess state that has any substantial overlap with the desired state. The algorithm would fail in this case. In our algorithm, the initial state does not need to have a large overlap with any particular state. As mentioned above, the observation of a transition in the probe signals a corresponding transition in the system. The post-transition state can now be treated as the initial state for the next step in the algorithm. This way, one can guide the system to any energy eigenstate, including the ground state. The freedom in choosing the operator A allows additional controllability for this purpose.

We note here that there is no single choice of the operator A that is needed in order to obtain a certain energy difference, say between the ground state and first-excited state. As explained above, it should be possible to go from any state to any other state via a relatively small number of intermediate states. An exception might be glassy and similar frustrated systems with a large number of vastly different low-energy states. However, there is no known efficient algorithm, classical or quantum, for exhaustively identifying the low-energy states of such complex systems.

In the PEA, one needs to have a good idea about the form of the energy eigenstates of interest. In our algorithm no such a priori knowledge is needed. If one is interested in the low-energy spectrum, the relevant states would show up naturally in the spectrum. This property is demonstrated in the example, showing that our algorithm can work in cases where the PEA fails.

In the PEA, one obtains the absolute eigenenergy of the system. For a large system, the absolute eigenenergy

could be a large number, much larger than the separation between the energy eigenstates of interest. This large overall energy would appear as part of the output, thus taking up resources such as additional index qubits. In our algorithm, one obtains the energy difference between energy levels, therefore avoiding the unnecessary readout of any overall energy shift. Note that the number of qubits required for implementing our algorithm is the same as that in the optimized version of the PEA [8, 20].

V. CONCLUSION

We have presented a hybrid analogue/digital quantum algorithm for obtaining the energy spectrum of a physical system. The algorithm provides more flexibility than the phase estimation algorithm. It can also be used to simulate a realistic interaction, and naturally identify transitions that would occur in a realistic setting. The algorithm can also be used to prepare any desired energy eigenstate of a physical system.

Acknowledgments

We acknowledge partial support from DARPA, AFOSR, ARO, NSF grant No. 0726909, JSPS-RFBR contract No. 12-02-92100, Grant-in-Aid for Scientific Research (S), MEXT Kakenhi on Quantum Cybernetics, and the JSPS FIRST program. HW is supported by “the Fundamental Research Funds for the Central Universities” of China.

-
- [1] D. Bacon and W. van Dam, *Communications of the ACM*, **53**, 84 (2010).
 - [2] M.-H. Yung, J. D. Whitefield, S. Boixo, D. G. Tempel and A. Aspuru-Guzik, e-print arXiv:1203.1331 (2012).
 - [3] J. Yopez and B. Boghosian, *Comp. Phys. Comm.* **146**, 280-294 (2002).
 - [4] I. Buluta, F. Nori, *Science* **326**, 108 (2009).
 - [5] I. Buluta, S. Ashhab, F. Nori, *Rep. Prog. Phys.* **74**, 104401 (2011).
 - [6] A. Y. Kitaev, e-print arXiv: quant-ph/9707021, 1997.
 - [7] D. S. Abrams and S. Lloyd, *Phys. Rev. Lett.* **83**, 5162 (1999).
 - [8] A. Aspuru-Guzik, A. D. Dutoi, P. J. Love, and M. Head-Gordon, *Science* **309**, 1704 (2005).
 - [9] H. Wang, S. Kais, A. Aspuru-Guzik, and M. R. Hoffmann, *Phys. Chem. Chem. Phys.* **10**, 5388 (2008).
 - [10] H. Wang, L.-A. Wu, Y.-X. Liu, F. Nori, *Phys. Rev. A*, **82**, 062303 (2010).
 - [11] A. M. Childs and W. van Dam, *Rev. Mod. Phys.* **82**, 1 (2010).
 - [12] L.F. Wei, F. Nori, *J. of Phys. A* **37**, 4607 (2004).
 - [13] H. Wang, L.-A. Wu, Y.-X. Liu, F. Nori, *Phys. Rev. A* **82**, 062303 (2010).
 - [14] B. M. Terhal and D. P. DiVincenzo, *Phys. Rev. A*, **61**, 022301 (2000).
 - [15] H. Wang, S. Ashhab and F. Nori, *Phys. Rev. A*, **83**, 062317 (2011).
 - [16] N. Wiebe, D. W. Berry, P. Hoyer, B. C. Sanders, e-print arXiv:1011.3489 (2011).
 - [17] M. Nielsen, I. Chuang, *Quantum Computation and Quantum Information* (Cambridge Univ. Press, Cambridge 2000).
 - [18] A. Szabo, N. Ostlund, *Modern Quantum Chemistry: Introduction to advanced Electronic Structure Theory* (McGraw-Hill, New York, 1989).
 - [19] A. Kitaev, A. H. Shen, and M. N. Vyalyi. *Classical and quantum computation, Graduate studies in Mathematics* Vol. **47**. American Mathematical Society, Providence, RI, 2002.
 - [20] R. B. Griffiths and C.-S. Niu, *Phys. Rev. Lett.* **76**, 3228 (1996).